Environmental Pollution 205 (2015) 385–393

Contents lists available at ScienceDirect

Environmental Pollution

journal homepage: www.elsevier.com/locate/envpol

Different routes, same pathways: Molecular mechanisms under silver ion and nanoparticle exposures in the soil sentinel *Eisenia fetida*

Marta Novo [a, *], Elma Lahive [b], María Díez-Ortiz [b], Marianne Matzke [b], Andrew J. Morgan [a], David J. Spurgeon [b], Claus Svendsen [b], Peter Kille [a]

[a] Organisms and Environment Division, Cardiff School of Biosciences, Cardiff University, Cardiff, CF10 3AT, UK
[b] Centre for Ecology and Hydrology, Maclean Building, Wallingford, Oxfordshire, OX10 8BB, UK

ARTICLE INFO

Article history:
Received 18 April 2015
Received in revised form
3 July 2015
Accepted 7 July 2015
Available online 20 July 2015

Keywords:
Silver
Nanoparticles
Ions
Soil sentinel
Cryptic lineage
Toxicokinetics

ABSTRACT

Use of nanotechnology products is increasing; with silver (Ag) nanoparticles particularly widely used. A key uncertainty surrounding the risk assessment of AgNPs is whether their effects are driven through the same mechanism of action that underlies the toxic effects of Ag ions. We present the first full transcriptome study of the effects of Ag ions and NPs in an ecotoxicological model soil invertebrate, the earthworm *Eisenia fetida*. Gene expression analyses indicated similar mechanisms for both silver forms with toxicity being exerted through pathways related to ribosome function, sugar and protein metabolism, molecular stress, disruption of energy production and histones. The main difference seen between Ag ions and NPs was associated with potential toxicokinetic effects related to cellular internalisation and communication, with pathways related to endocytosis and cilia being significantly enriched. These results point to a common final toxicodynamic response, but initial internalisation driven by different exposure routes and toxicokinetic mechanisms.

1. Introduction

Silver (Ag) is amongst the most toxic of all metals, with a relatively high reported potency towards both invertebrates (e.g., Bianchini et al., 2005) and vertebrates (e.g., Hogstrand and Wood, 1998). Prior to the advent of modern antibiotics the wide-spectrum antimicrobial efficacy of Ag^+ ions was harnessed to produce effective biocides for medical applications (Davenport and Keeley, 2005; Lansdown, 2006; Kollef et al., 2008). These applications rely on the production and release of Ag^+ ions from the otherwise inert surface that is in contact with the target biofilm; this produces a localised elevation in the concentration of Ag^+ ions resulting in an effective anti-microbial activity. The increase in surface area afforded by Ag nanoparticles (AgNPs) creates a more efficient dissolution of Ag^+ ions that has potential use for personal care, household, clothing and medical applications (e.g., Wilkinson et al., 2011). This increasing range of uses is expected to result in increased releases to the environment including soil.

Physical factors underpinning AgNPs dissolution, and production of Ag^+ ions, are central to determining the relative toxicity of the particle to receptor organisms. Such processes include, but are not limited to changes in surface speciation (e.g. sulfidation), coating form and aggregation dynamics (Lowry et al., 2012). The extent to which these processes ultimately determine exposure and toxicity is also dependent on the receptor organism physiology (Tourinho et al., 2012). Traits such as intestinal conditions (including the microbiome), cell surface chemistries, activity of the endocytic pathways and route of metal handling will all influence the levels of AgNP and Ag ion exposure and internalisation as well as the resulting mechanisms and extent of toxicity.

To date the mechanistic effects of AgNP have been studied mostly in classic laboratory model organisms including *Caenorhabditis elegans*, *Daphnia* or *Danio rerio* (e.g. (Roh et al., 2009; Poynton et al., 2011, 2012; van Aerle et al., 2013)). Moreover the majority of the investigations has been directed towards aquatic environments (e.g. (Poynton et al., 2011; van Aerle et al., 2013; Farkas et al., 2011)) leaving studies for terrestrial sentinel species largely neglected. Earthworms are used as a model species for terrestrial ecotoxicology studies, selected because of their key role as ecosystem engineers. Several studies on the effect of NPs on cytotoxicity (Kwak et al., 2014), reproduction (Schlich et al., 2013), behaviour (Shoults-Wilson et al., 2011) and molecular stress

* Corresponding author.
E-mail address: novom@cf.ac.uk (M. Novo).

http://dx.doi.org/10.1016/j.envpol.2015.07.010

(Tsyusko et al., 2012a; Hayashi et al., 2013) in earthworms are available. However, these studies have not evaluated the holistic impact of AgNPs exposure, but instead focused on specific biological endpoints or pathways. Transcriptomic studies in earthworms have the potential to elucidate such holistic effects (e.g., Owen et al., 2008; Gong et al., 2010; Bundy et al., 2008). However, emerging evidence of deep cryptic genetic speciation within earthworms (e.g. King et al., 2008; Novo et al., 2009, 2010; Buckley et al., 2011; James et al., 2010; Cunha et al., 2014) highlights potential problems with previous approaches due to the risk of conflating the toxicological responses of divergent lineages (Dallinger and Hockner, 2013; Otomo et al., 2013). For these reasons care in the selection of tested organisms for transcriptional analysis, coupled with the use of newer sequencing based methods are needed to meet the challenges of unambiguously identifying the overall comparative effects of AgNPs and ions. Here we report the results of a toxicogenomic study for AgNPs and Ag^+ ions in the earthworm *Eisenia fetida*. Our aims were first to generate a comprehensive transcriptome for this ecotoxicological model soil invertebrate, and second, to investigate the mechanistic effects of AgNPs and Ag^+ ions on this transcriptome after exposure, identifying common and different pathways affected by the different silver forms within a wide systems biology context for earthworms. Selection of individuals from a single lineage, coupled with the use of an RNA-seq analysis is used to compare the pathway responses to AgNPs and Ag^+ ions at a similar effect level (EC_{50} for reproduction) to elucidate whether there is evidence for any AgNP specific uptake or response pathways.

2. Materials and methods

2.1. Material supply and characterisation

The 50 nm AgNPs were obtained from Institut Català de Nanotecnología (ICN) (Barcelona, Spain). The materials were supplied as spherical nanoparticles with a documented diameter of 50 nm. AgNPs with a purity of 40.6% Ag was coated with polyvinylpyrrolidone with average mol wt 10,000 (PVP-10 K). The particles were lyophilised from a solution containing sodium citrate and tannic acid included as stabilizers and protective molecules and supplied in powder form including these molecules.

To reconfirm the stated primary particle morphology, size and assess potential aggregation status prior to use, dispersions of the AgNPs were prepared in distilled water at 1 mg/ml and sonicated at room temperature for 1 min. The hydrodynamic diameter and zeta potential of the AgNPs in this stock suspension was measured with Malvern ZetaSizer Nano ZS. Samples were also visualised using transmission electron microscopy (TEM) on a JEOL 1010 analytical. For these assessments, samples taken from the stock suspension were dispersed in water and a drop of the dispersion deposited on a holey carbon coated Cu-TEM grid and dried at room temperature for several hours. $AgNO_3$ salt used for the ionic exposures was purchased from BHD Chemicals (Poole, UK) as a white crystalline powder.

2.2. Earthworm toxicity test

The AgNP and $AgNO_3$ earthworm exposures were conducted in a loamy sand soil (LUFA-Speyer 2.2, LUFA, Germany). See details for soils in Supporting Information (SI) S1. To establish earthworm sensitivity and to prepare worms for the RNA-seq analysis, earthworms were exposed in soils spiked with coated AgNPs and $AgNO_3$ at seven concentrations (0, 18, 45, 112, 281, 703 and 1758 mg Ag kg^{-1} dry weight). Concentrations were measured following Diez-Ortiz et al. (2015). Direct dry dosing of both Ag forms into the soil followed by thorough mixing of the dry soils was selected as the best approach for dosing. This has been shown to produce a homogenous NP distribution in the soil and similar exposure to aqueous dosing, while being less technically challenging to achieve a reliable addition (see (Waalewijn-Kool et al., 2013)). Immediately after dosing, pure MilliQ water was added to all soil batches to reach 45% of the WHC and soils were again thoroughly mixed to ensure a homogeneous Ag distribution. Soils were then incubated for one week to allow the soil chemistry to reach an initial equilibrium after dosing before the earthworms were added.

Toxicity studies followed the OECD standard reproductive toxicity test for the earthworm *E. fetida* (OECD 222 (OECD, 2004)). In brief, the earthworms were incubated in the soil for 28 days after which the soils were hand-sorted and surviving worms collected, counted and weighed. The worms for transcriptome analysis were flash frozen in liquid nitrogen and stored at −80 °C. Soils were then returned to the test boxes for a further four week incubation to allow cocoon hatching. For details of the toxicity tests see SI-S1. From the survival and juvenile count data, 28 days LC_{50} and 56 day $EC50_{reproduction}$ values (and 95% CI) were derived using a logistic model (Haanstra et al., 1985) fitted in SPSS 17.0.

2.3. Earthworms for transcriptome analysis

Earthworms for transcriptomic analysis were taken from the treatment closest to the derived $EC50_{reproduction}$ for AgNP and $AgNO_3$ to ensure comparisons were made at the same effect level. Earthworms were crushed in liquid nitrogen and DNA extracted from 25 mg of tissue. DNAeasy Tissue Kit (QIAGEN) protocol was followed. Because of potential for crypsis in *E. fetida*, all individuals were first genotyped for the mitochondrial gene cytochrome c oxidase subunit I (COI) to ensure that only earthworms from the same lineage were further processed. See details for PCR reaction in SI-S1. We also included sequences from individuals of different exposure experiments from our laboratory in order to have a clear overview of genetic variability. Additionally *E. fetida* and *Eisenia andrei* sequences were downloaded from GenBank with two Lumbricids and one Hormogastridae added to the data-set as outgroup (SI-S2). A Bayesian Phylogeny was estimated and pairwise genetic distances were measured (details in SI-S1). Individuals from a single lineage were then selected from the control and treatments for the RNA-seq analysis.

2.4. Construction and annotation of a reference transcriptome

A reference transcriptome representing the integration of data from both control and exposed organisms was assembled from the RNA-seq data following the scheme illustrated in Fig. 1. Samples used for generation of the reference transcriptome were taken from across a range of control and nanoparticle exposures, as well as individuals of different life-stages (hatching, mid-log growth phase juveniles, subadults) from the culture population. All worms used were powdered under liquid nitrogen. See details of RNA extraction protocol in SI-S1. Equal amounts of five samples representing different developmental stages and a range of NP exposures were combined in a single tube (SI-S2) and a cDNA library constructed by BaseClear (www.baseclear.com) following Tru-Seq (Illumina) protocol and sequenced on Illumina Hi-Seq 2000 using a 50 cycle paired ended protocol.

Transcriptomes for AgNP and Ag ion exposed samples were generated for separate individuals from true biological replicate containers at the treatment closest to the respective AgNP and Ag ion $EC50_{reproduction}$ and the control (one earthworm per replicate, three replicates per treatment). All the selected earthworms were closely related and the p-distance for the most distant sample (HAP-60) was 1.1%. Haplotypes are shown in SI-S2. RNA was extracted and 9 libraries were prepared and multiplexed for sequencing as above but using a 50 cycle single ended protocol which was designed to yield a minimum of 20 million reads per sample.

The data was initially checked for base quality and filtered for data passing the Illumina Chastily default parameters. Sequences containing adapters and/or PhiX control signal were removed with a filtering protocol by BaseClear. *In silico* normalization was conducted by Trinity v. r2013-02-25 (Grabherr et al., 2011) using both paired and single end data. To achieve the most complete baseline transcriptome, we additionally included single reads from a RNA-seq analysis of Zn exposure experiment (Authors' unpublished data). A subsequent assembly was performed using Trinity under default settings using the combined normalised data. The resultant contigs were annotated by blastX analysis against Uniprot database filtering for hits with an e-value $<1e^{-5}$.

2.5. Quantitative transcriptomic analysis

Sequence reads (50 bp) generated from the 9 exposure samples were mapped against the reference transcriptome using Bowtie1 (Langmead et al., 2009) allowing three mismatches (-v 3) and retrieving only uniquely mapped reads (m -1). Statistical analyses were performed in EdgeR (Robinson et al., 2010). Contigs where the observed frequency of mapped reads per million fell below 1 for all the replicates within a specific group were removed from subsequent analysis. Exact tests were performed for each of the comparisons (i.e. NP *vs.* control; ion *vs.* control; NP *vs.* ion) and the differentially expressed transcripts detected (applying a False Discovery Rate FDR 10%) were further used to conduct enrichment analyses in DAVID (Huang et al., 2009). Finally, results from the enrichment analyses were visualized and interpreted in cytoscape 2.8.2 (Smoot et al., 2011) using the plugin Enrichment Map v 1.2 (Merico et al., 2010) with default settings (*p*-value Cutoff 0.005, FDR Q-value Cutoff 0.1). A full analysis workflow is presented in Fig. 1.

3. Results

See material characterization and concentration validation in SI-S1.

3.1. Exposures

There was >90% survival of *E. fetida* in soil spiked with PVP-coated AgNP at concentrations up to 1758 mg Ag/kg d.w. and for Ag ions at treatments up to 113 A g/kg d.w. Higher ionic treatments resulted in reduced survival and no earthworms survived exposure

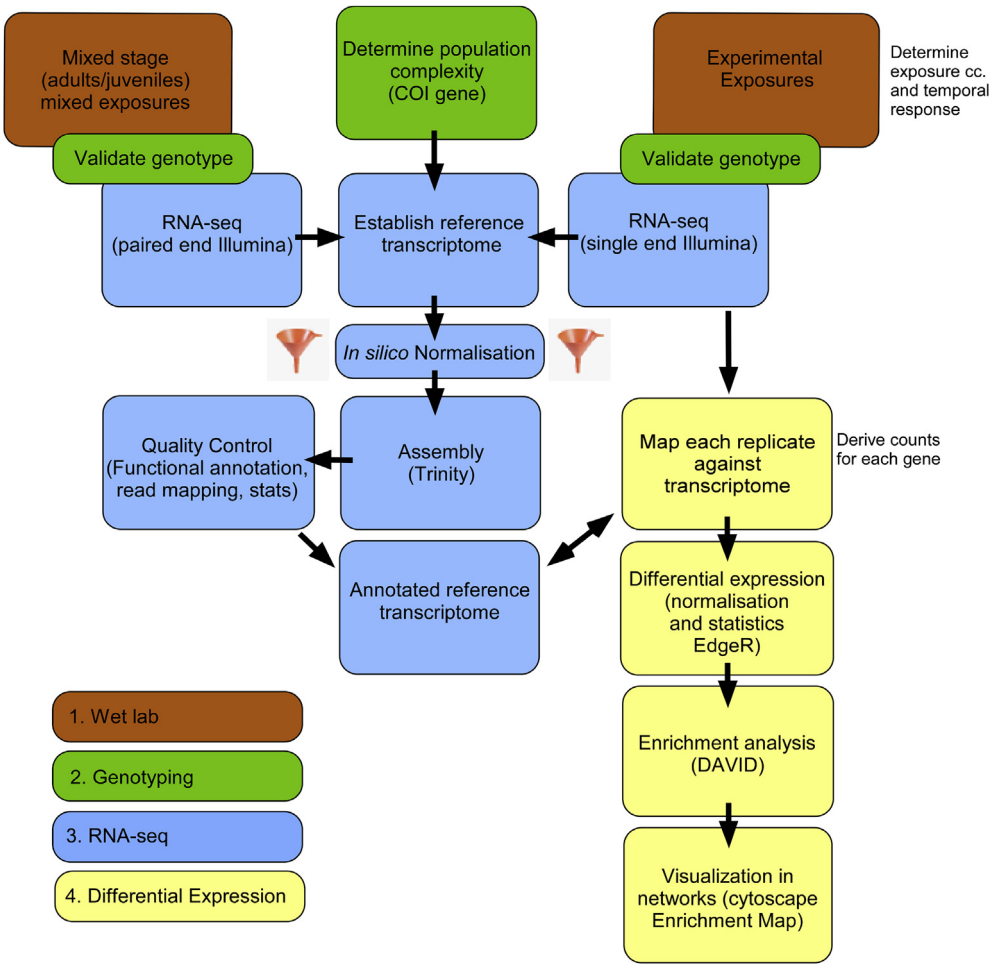

Fig. 1. Representation of the workflow followed in the present study showing the steps for wet lab, genotyping, RNA-seq transcriptome assembly and quantitative analysis.

to 703 mg Ag/kg d.w. and above. Earthworm reproduction was reduced in a dose-dependent manner following exposure to both Ag forms. The EC_{50} values 445 (95% CI, 196–695) and 49 (95% CI, 46–51) mg Ag/kg d.w. were estimated for the earthworms exposed to soils spiked with PVP AgNP and Ag ions, respectively. The exposure concentrations closest to the $EC_{50,\ reproduction}$ and therefore selected for transcriptome analysis, were 281 mg Ag/kg d.w for AgNPs and 45 mg Ag/kg d.w for Ag ions.

3.2. Genotyping

All sequences have been deposited in GenBank (Accession numbers: KP236544–KP236587). We found a significant heterogeneity among the COI sequences (Fig. 2, SI-S2). Two main groups of haplotypes or lineages were present. Between lineages uncorrected p-distance values were up to 15%. More distant isolated haplotypes were represented by both specimens from the present study as well as database accessions with these additional haplotypes increasing the p-distances up to 17.3%. Among GenBank sequences only those assigned to *E. fetida* appeared within the upper lineage (Fig. 2), whilst sequences representing both *E. fetida* and *E. andrei* appeared together within the lower lineage with some haplotypes putatively derived from the two different species.

3.3. Reference transcriptome and RNA-seq

Reads have been submitted to the European Nucleotide Archive (ENA) under the study number PRJEB7919. The number of reads used for reference transcriptome assembly after the quality trimming was ca. 32 million for the paired end sequences and ca. 660 million for the single end reads. The Trinity normalised assembly yielded a N50 of 1259 and 30,932 contigs longer than 1000 bp (SI-S3). The number of contigs yielding a significant Blast match was 37,499, although number of non-redundant hits was 16,505.

Around 76% of the reads from each sample mapped against the reference transcriptome, and 47.06–51.99% of the reads uniquely mapped and therefore were informative for subsequent quantitative analyses.

Paired comparisons (FDR 10%) of; (i) Ag ion *vs.* control yielded 529 down-regulated and 618 up-regulated transcripts; (ii) AgNPs *vs.* control resulted in 237 down-regulated and 454 up-regulated transcripts; and (iii) AgNP *vs.* Ag ion showed 449 down-regulated and 758 up-regulated transcripts (see SI-S4, S5, S6 for lists of differentially expressed genes and significant BLAST hits).

3.4. Common pathways affected by NP and ions

The comparison of genes significantly changing in expression compared to controls in earthworms exposed to the AgNPs and Ag ions indicated a large degree of overlap, with 175 genes with blast hit shared between the two gene lists (see Fig. 3A). The most significant enrichment results for earthworms exposed to the AgNPs and Ag ions were summarised as networks (Fig. 3, Table 1). This analysis highlighted commonly affected pathways for the effects of Ag ions (Fig. 3B) and AgNPs (Fig. 3C) exposure. These impacted pathways related to overall energy metabolism through genes

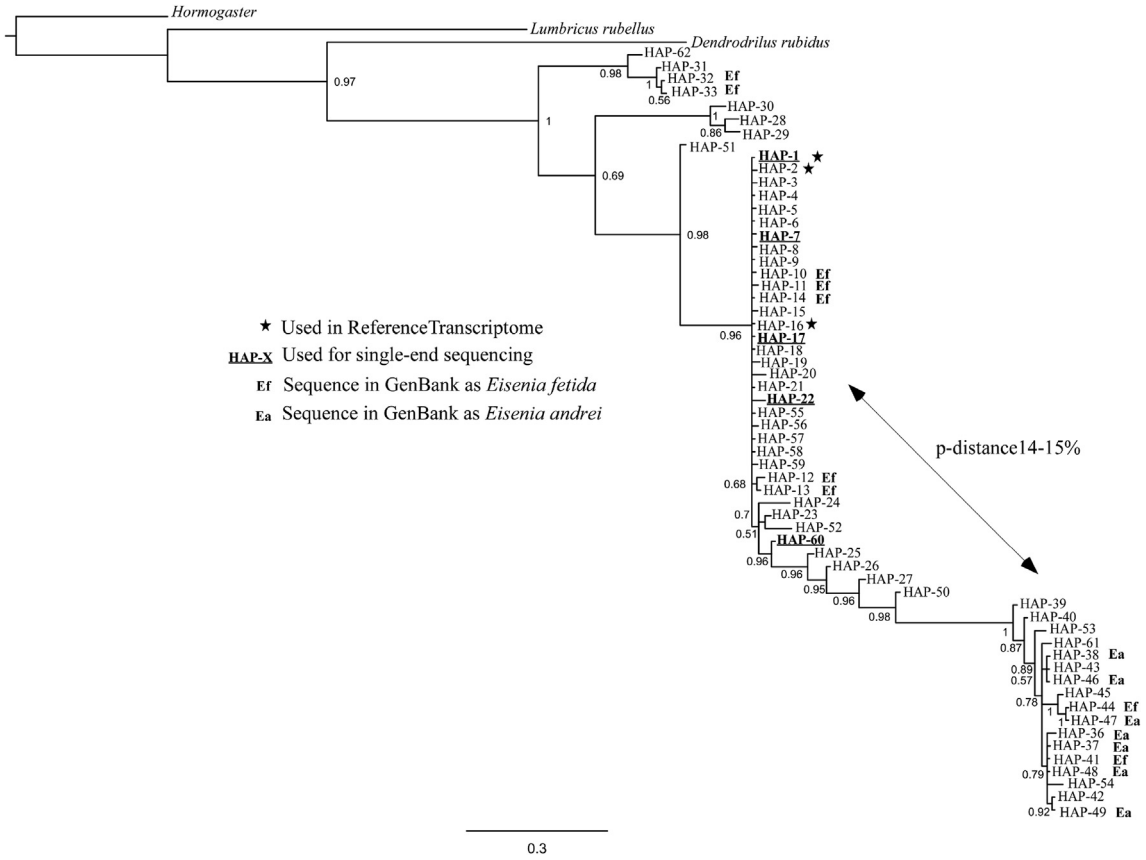

Fig. 2. Bayesian phylogenetic tree based on COI sequences from *Eisenia fetida* from our experiments and sequences retrieved from GenBank (see SI-S2). Posterior probability values higher than 0.5 are shown on the nodes or below branches.

involved in sugar metabolism and adenylate kinase activity; protein and amino acid turnover through genes involved in amino acid metabolism and ribosomal activity and effects on DNA through genes integral to the nucleosomes, as well as a small number of additional pathways for the AgNPs for oxidoreductase activity and metal ion responses (SI-S4, S5, S7, S8).

Upregulation of gene encoding enzymes that are implicated in glycolysis, gluconeogenesis and citric acid cycle, such as malate, pyruvate, alcohol and succinate dehydrogenases, fructose biphosphate aldolase, galactokinase, phosphoglycerate kinase, reflect the changes in sugar metabolism (full list of genes in SI-S4, S5). Common significant changes in genes related to mitochondrial electron transport and oxidative stress further extend these shared responses.

The common effects on pathways related to amino acid and protein metabolism are driven by significant upregulation of genes encoding enzymes implicated in the amino acid biosynthetic process such as ornithine carbamoyltransferase, glutamine synthetase or L-threonine dehydratase biosynthetic IlvA. There are a number of genes encoding ribosomal sub-units significantly upregulated in both Ag exposures, as were genes encoding heat shock proteins, specifically HSP70 and HSP90, involved in chaperoning as a component part of protein turnover. Structural development of the cell cytoskeleton by both Ag forms was indicated by genes such as elongation factors and tubulin, a major component of cell microtubules as well as upregulation of caltractin, a calcium binding protein involved in microtubule structure and function. The effects on the nucleosomes are driven through upregulation of histones 2, 3 and 4 and on translation-initiation factors.

3.5. Differences in the transcriptional effects between Ag NP and Ag ion exposures

Significantly enriched pathways between NP and ion treatments related to endocytosis and cilia (Fig. 3D, Table 2). Other pathways including differentially expressed genes showing a lower degree of enrichment included meiosis, sexual reproduction and gamete formation and differentiation or excretion (SI-S6, S9).

Within the effects related to endocytosis significant changes were seen for pathways associated with basal lamina, laminin, basolateral plasma membrane, extracellular region and microtubules. Earthworms exposed to AgNPs showed upregulation of the genes coding for different cell structural units including heavy and intermediate chains of dynein, laminin subunits and collagen compared to earthworms exposed to Ag ions. Cell growth factors including angyopoietin, midkine and wnt-4 and gene encoding aquaporin, solute carriers and zinc metalloproteinase were also upregulated. Genes downregulated in the NP exposures included membrane proteins such as the LDL lipoprotein receptor-related protein and peripheral membrane protein CASK and key genes in developmental programming such as netrin and wech protein.

The cilia associated enriched components included pathways related to axoneme, dynein complex, cell projection, microtubule and cilium. Compared to the ion exposure, AgNP exposure caused upregulation of different heavy and intermediate chains of dynein, as well as cubilin, sperm specific protein Don juan, V-type proton ATPase, polycystin, neurotrypsin, while peripheral plasma membrane protein (CASK), Rab effector MyRIP and LDL lipoprotein receptor-related protein among others were all significantly downregulated.

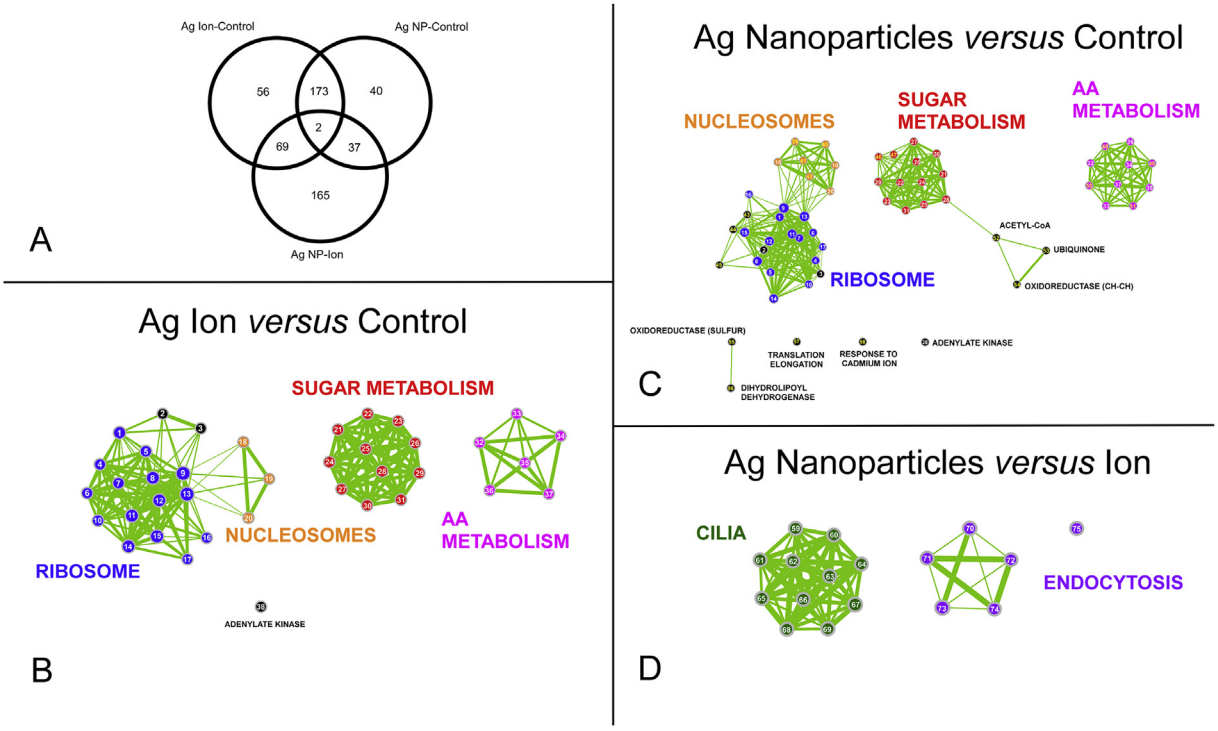

Fig. 3. Panel A shows a Venn diagram of the overlapping genes among the three comparisons (only genes with blast hit were included). Panels B, C, D: Go-term networks generated by cytoscape after enrichment analyses in DAVID (P-value Cutoff 0.005, FDR Q-value Cutoff 0.1). When comparing B and C white numbers indicate common terms in both and yellow numbers indicate exclusive terms for C. Go-terms represented by those numbers are shown in Table 1 (For interpretation of the references to colour in this figure legend, the reader is referred to the web version of this article).

4. Discussion

Many studies have measured both the toxicity of metal and metal oxide NPs and their constituent ions. A recent meta-analysis of these comparative studies has shown that in 93.8% of case for Ag, 100% for Cu and 81% for Zn the nano-form is less toxic than the dissolved metal when compared on a total metal mass concentration basis (Notter et al., 2014). Indeed the toxicity tests conducted as a prelude to the RNA-seq mechanistic assessment in this present paper confirm this pattern for the PVP coated AgNPs tested. The trends for reduced toxicity of metal and metal oxide based NP compared to ionic forms on a mass basis is likely to be driven to a large extent by the differences in environmental availability of metal ions for uptake between the two metal forms (Heggelund et al., 2014). However, it is also possible that differences in the toxicokinetics and toxicodynamics of the added metal forms in different organisms may also play a role. The potential for increased uptake of nanoparticles by some species, such as filter feeders, has already been recognised (Baker et al., 2014). However, what remains less clear is whether once in the body the metal derived from uptake of intact NPs have the same internal fate and exert toxicity through the same mechanisms of action as uptake of ionic species of the same metal. Transcriptional analysis using high coverage techniques such as RNA-seq are a comprehensive way to address this key uncertainty.

4.1. Importance of genotyping

The species *E. fetida* and *E. andrei* have been widely used as standard laboratory test organisms for studies in applied ecology and toxicology (e.g. (Kwak et al., 2014) and references). *E. fetida* has already been used for transcriptomic studies (Tsyusko et al., 2012a; Hayashi et al., 2013); however, recent evidence pointing to deep cryptic speciation in earthworms has the potential to confound such analysis. In most terrestrial ecotoxicology laboratories, the animals used are taken from long-standing culture stocks or provided by commercial suppliers. Until recently, these stocks have not been genotyped prior to use (but see Römbkea et al., 2015).

To avoid confounding our analysis by including genetically divergent individuals, we initially genotyped all worms exposed to the selected concentration for RNA-seq. Analysis of the COI locus indicated a genetic mixture in our cultures, with two main lineages showing an uncorrected p-distance of about 15%, but also distant haplotypes with divergences up to 17.3%. Sequences retrieved from GenBank and identified there as *E. fetida* and *E. andrei*, but clustered together in our phylogenetic tree showing a problem in identification of these species. This issue was most prevalent in the lower lineage group of Fig. 2, where both *E. fetida* and *E. andrei* sequences were placed. Confusion over the taxonomy of species in the *E. fetida*/*E. andrei* complex has existed for some time, arising because these earthworms are morphologically very similar. Nonetheless, they are widely accepted as different phylogenetic species and Perez-Losada et al. (2005) suggest the further presence of cryptic species within *E. fetida*. Our analysis confirms there is indeed a deep cryptic speciation in morphotype *E. fetida* that needs to be considered when designing toxicity test programs and in particularly sequencing based mechanistic studies due to the potential for reference transcriptome construction and read alignments to be confounded if earthworms from different lineages are individually used and results compared.

4.2. Transcriptome for toxicology sentinel and its response to different Ag forms

A well-represented transcriptome for *E. fetida* has been assembled. This resource will aid future applied investigation in soil environments by providing a very rich source of information to enable use of second generation sequencing to promote a research line

Table 1
Enrichment results from DAVID analyses identified as the most significant by cytoscape (see networks in Fig. 3 with coincident numbers of the nodes) for paired comparisons NP and ion *vs* control. See complete results of the enrichment analyses in SI-S7 and S8 and complete gene lists in SI-S4 and S5.

			Ion_*vs*_control		NP_*vs*_control	
Node	Term	Category	PValue	Fold Enrichment	PValue	Fold Enrichment
	RIBOSOME					
1	GO:0005829~cytosol	CC	1,70E-05	2,24	5,20E-07	2,66
4	GO:0015935~small ribosomal subunit	CC	2,34E-18	20,90	3,15E-23	28,43
5	GO:0033279~ribosomal subunit	CC	1,21E-17	14,02	2,68E-22	18,79
6	GO:0022627~cytosolic small ribosomal subunit	CC	1,29E-18	28,15	9,78E-24	38,76
7	GO:0022626~cytosolic ribosome	CC	4,29E-21	22,33	2,86E-26	30,07
8	GO:0030529~ribonucleoprotein complex	CC	6,49E-22	5,28	2,33E-30	7,00
9	GO:0043228~non-membrane-bounded organelle	CC	7,72E-07	1,80	5,38E-12	2,27
10	GO:0044445~cytosolic part	CC	1,53E-12	10,05	1,62E-16	13,67
11	GO:0006412~translation	BP	3,37E-26	7,20	5,81E-34	8,91
12	GO:0005840~ribosome	CC	6,69E-34	11,41	2,32E-42	14,91
13	GO:0043232~intracellular non-membrane-bounded organelle	CC	7,72E-07	1,80	5,38E-12	2,27
14	GO:0003735~structural constituent of ribosome	MF	7,08E-33	11,97	7,31E-40	14,92
15	GO:0005198~structural molecule activity	MF	1,92E-24	6,03	1,23E-28	7,15
16	GO:0006414~translational elongation	BP	7,66E-09	11,08	1,49E-10	13,41
17	GO:0019843~rRNA binding	MF	7,00E-07	14,90	2,50E-07	17,33
	NUCLEOSOMES					
18	GO:0000786~nucleosome	CC	2,62E-04	15,28	1,20E-04	18,70
19	GO:0032993~protein-DNA complex	CC	4,97E-04	8,93	2,05E-03	9,11
20	GO:0006334~nucleosome assembly	BP	1,13E-03	10,60	7,48E-04	11,84
39	GO:0031497~chromatin assembly	BP	2,44E-03	8,68	1,62E-03	9,69
40	GO:0065004~protein-DNA complex assembly	BP	2,44E-03	8,68	1,62E-03	9,69
41	GO:0034622~cellular macromolecular complex assembly	BP	5,92E-03	2,80	2,70E-03	3,13
42	GO:0034728~nucleosome organization	BP	2,72E-03	8,42	1,82E-03	9,40
	SUGAR METABOLISM					
21	GO:0006006~glucose metabolic process	BP	3,98E-08	6,19	1,06E-09	7,35
22	GO:0016052~carbohydrate catabolic process	BP	3,41E-10	7,91	6,41E-11	8,84
23	GO:0044275~cellular carbohydrate catabolic process	BP	2,95E-10	9,76	4,77E-12	11,63
24	GO:0019318~hexose metabolic process	BP	1,78E-08	5,63	4,33E-10	6,64
25	GO:0046365~monosaccharide catabolic process	BP	1,43E-11	12,10	1,73E-13	14,41
26	GO:0046164~alcohol catabolic process	BP	1,55E-10	10,22	2,35E-12	12,18
27	GO:0006096~glycolysis	BP	1,39E-11	13,82	1,57E-13	16,54
28	GO:0006091~generation of precursor metabolites and energy	BP	3,12E-07	4,15	1,66E-09	5,10
29	GO:0005996~monosaccharide metabolic process	BP	1,10E-07	4,98	3,21E-09	5,87
30	GO:0019320~hexose catabolic process	BP	9,47E-12	12,45	1,10E-13	14,83
31	GO:0006007~glucose catabolic process	BP	7,66E-12	12,63	8,71E-14	15,05
46	GO:0004332~fructose-bisphosphate aldolase activity	MF	3,49E-03	31,30	2,59E-03	36,39
47	GO:0016774~phosphotransferase activity, carboxyl group as acceptor	MF	no	no	4,78E-04	24,26
	AA METABOLISM					
32	GO:0009082~branched chain family amino acid biosynthetic process	BP	1,72E-04	32,72	1,23E-04	36,54
33	GO:0008652~cellular amino acid biosynthetic process	BP	1,43E-03	5,65	1,34E-05	8,11
34	GO:0004794~L-threonine ammonia-lyase activity	MF	2,26E-04	29,81	1,44E-04	34,66
35	GO:0006549~isoleucine metabolic process	BP	4,01E-04	25,45	2,89E-04	28,42
36	GO:0009097~isoleucine biosynthetic process	BP	9,93E-05	38,17	7,13E-05	42,64
37	GO:0016841~ammonia-lyase activity	MF	1,01E-03	18,97	6,49E-04	22,06
48	GO:0016053~organic acid biosynthetic process	BP	2,74E-03	3,39	3,02E-04	4,16
49	GO:0046394~carboxylic acid biosynthetic process	BP	2,74E-03	3,39	3,02E-04	4,16
50	GO:0016840~carbon-nitrogen lyase activity	MF	3,82E-03	12,27	2,49E-03	14,27
51	GO:0009309~amine biosynthetic process	BP	1,33E-02	3,58	3,49E-04	5,14
	UNCLASSIFIED					
2	GO:0030312~external encapsulating structure	CC	5,99E-08	15,84	1,21E-08	19,38
3	GO:0005618~cell wall	CC	2,64E-08	17,42	5,30E-09	21,32
38	GO:0004017~adenylate kinase activity	MF	1,33E-03	17,39	8,55E-04	20,22
43	GO:0009536~plastid	CC	6,78E-03	10,10	2,62E-04	15,45
44	GO:0009507~chloroplast	CC	5,22E-03	11,06	1,81E-04	16,92
45	GO:0005773~vacuole	CC	2,97E-02	2,30	2,82E-03	3,09
52	GO:0006084~acetyl-CoA metabolic process	BP	2,79E-02	6,03	2,76E-03	8,41
53	GO:0008177~succinate dehydrogenase (ubiquinone) activity	MF	no	no	3,84E-03	30,33
54	GO:0016635~oxidoreductase activity, acting on the CH-CH group of donors, qui	MF	no	no	3,84E-03	30,33
55	GO:0016667~oxidoreductase activity, acting on sulfur group of donors	MF	4,29E-02	5,09	4,41E-03	7,40
56	GO:0004148~dihydrolipoyl dehydrogenase activity	MF	2,12E-03	39,12	1,57E-03	45,49
57	GO:0003746~translation elongation factor activity	MF	2,45E-02	6,32	1,97E-03	9,19
58	GO:0046686~response to cadmium ion	BP	2,93E-03	13,47	1,15E-04	18,81

Table 2
Enrichment results from DAVID analyses identified as the most significant by cytoscape (see networks in Fig. 3 with coincident numbers of the nodes) for paired comparison NP *vs* ion. See complete results of the enrichment analyses SI-S9 and complete gene lists in SI-S6.

			NP_*vs*_ion	
Node	Term	Category	PValue	Fold Enrichment
	CILIA			
59	GO:0005929~cilium	CC	2,62E-06	5,69
60	GO:0005930~axoneme	CC	1,69E-07	11,41
61	GO:0044441~cilium part	CC	1,85E-06	10,46
62	GO:0044447~axoneme part	CC	8,82E-05	19,97
63	GO:0005858~axonemal dynein complex	CC	1,70E-05	29,05
64	GO:0005875~microtubule associated complex	CC	1,80E-04	5,64
65	GO:0003777~microtubule motor activity	MF	1,63E-05	6,72
66	GO:0035085~cilium axoneme	CC	1,42E-07	14,38
67	GO:0042995~cell projection	CC	8,13E-06	2,77
68	GO:0030286~dynein complex	CC	7,41E-07	11,74
69	GO:0044463~cell projection part	CC	5,48E-05	4,22
	ENDOCYTOSIS			
70	GO:0044421~extracellular region part	CC	2,93E-03	2,21
71	GO:0005605~basal lamina	CC	4,56E-03	11,62
72	GO:0005606~laminin-1 complex	CC	5,54E-04	23,24
73	GO:0005576~extracellular region	CC	3,40E-03	1,77
74	GO:0043256~laminin complex	CC	7,30E-04	21,30
75	GO:0016323~basolateral plasma membrane	CC	2,62E-03	3,76

that has otherwise to date been based on microarray data and single gene studies (e.g., (Tsyusko et al., 2012a; Hayashi et al., 2013; Gong et al., 2010)). Using our reference transcriptome for read mapping and annotation, our results suggest that the two Ag forms (namely 50 nm PVP coated AgNPs and Ag ions; added as Ag nitrate). Apparently exert their toxicity through a similar set of biochemical pathways, although some differentiation was seen in the "exposure related" pathways affected (see details later). Thus, comparison of genes that were significantly changed in expression compared to control in both AgNPs and Ag ion exposed worms indicated a relative high overlap. A comprehensive pathway analysis indicated a significant enrichment for common pathways including those related to energy metabolism, protein turnover and DNA. Identification of a common mechanistic basis for the toxic effect of AgNPs and Ag ions in earthworms is consistent with the results of previous studies on the mussel proteome (Gomes et al., 2013) and fish transcriptome (Garcia-Reyero et al., 2014), as well as for single genes in earthworms (Tsyusko et al., 2012a). However, our results using whole transcriptome approach lets us extend the pathway-based analysis compared to these studies to include a fully quantitative assessment of the expression of the whole genome. This comprehensive approach extends the identification of a common response for silver forms to cover a wider systems biology context for earthworms. The pathways affected by exposure to both Ag forms provide a picture of the response of the earthworms to exposure at a toxic effect level that is consistent with previous observation for other metal ions (Owen et al., 2008; Bundy et al., 2008; Baylay et al., 2012). At exposure levels sufficient to cause a reduction in reproduction, large changes in the acquisition of energy resources from food and subsequent allocation to traits can be expected. Observation of changes in sugar metabolism and also genes involved in electron transport may reflect such effects. Bundy et al. (2008) successfully used a combined ^{1}H NMR and microarray based transcriptomic approach and identified an effect of copper on such energy related biochemical processes in earthworms. Similarly, Owen et al. (2008) identified an effect of Cd exposure on electron transport. These effects were linked to the targeting of these metals to the mitochondria and potential reactive oxygen species effects. The identification in this study of the effects of Ag exposure in both NP and ionic form on similar pathways appears to reflect the same vulnerability of energy metabolism in earthworms when exposed to toxicologically relevant concentrations of Ag, as for the Cu and Cd examples in the literature.

A second major group of pathways affected by exposure to both Ag forms were associated with protein metabolism including both ribosomal activity and also protein degradation as indicated by the significant upregulation of expression for the major protein chaperones HSP70 and HSP90. These effects on protein metabolism may occur as a consequence of the disruption to sugar metabolism described above, thereby, promoting protein use for metabolic purposes.

Alternatively, they may reflect the direct consequences of increased reactive oxygen species activity resulting from compromised electron transport on protein integrity, which may also underpin effects on the integrity of DNA including its associated histones. The observed effects of Ag exposure on DNA status is

consistent with previous findings for earthworms exposed to Cd ions (Owen et al., 2008). Further, there has been growing evidence to suggest changes in epigenetic marks can occur as a result of environmental exposure to metals including arsenic, cadmium, chromium and nickel (Martinez-Zamudio and Ha, 2011). Moreover some NPs, such as cadmium telluride quantum dots, have been shown to induce global hypoacetylation (Choi et al., 2008). Mechanisms by which Ag may interact with chromatin changes should be further investigated and could elucidate the mode of Ag toxicity and perhaps the potential for transgenerational effects.

4.3. Different uptake routes of AgNPs and Ag ions

The potential for the dissolution of AgNPs to derive Ag ions could be a cause of the observed shared effect. There is the potential for such dissolution to occur both externally in the test media (Fabrega et al., 2009; Cornelis et al., 2012) as well as following uptake. Information on internal Ag metal concentration would not alone be sufficient to establish the internal status of Ag assimilated in the NP exposure, as information would be needed on speciation. The pathway analysis of the genes differing in expression between the NP and ion exposed worms identified a significant enrichment for genes involved in endocytosis and cilia structures. Endocytosis has been previously highlighted as a possible route through which NPs can enter into tissues (Wilkinson et al., 2011; AshaRani et al., 2009). In the nematode *C. elegans*, worms mutant for rme-2, a gene known to be involved in endocytosis, showed lower sensitivity to gold NP than wild type worms, indicating a role for a vesicular pathway during uptake into nematodes (Tsyusko et al., 2012b). The enrichment for a range of key pathways involved in endocytosis (e.g. basal lamina, laminin, basolateral plasma membrane, extracellular region and microtubules) in the NP exposed earthworms in the present study suggests a similar role for this route in AgNP toxicokinetics in earthworms. The cause of the effect on genes involved in the function of the cell cilia is less clear. It has recently been (re)discovered that non-motile primary cilia, and some motile cilia, in invertebrates as well as vertebrates possess a basal membrane domain called the 'ciliary pocket', a structure postulated to be involved in clathrin-mediated endocytosis (Benmerah, 2013). Earthworms possess ciliated cells both in several regions of the alimentary epithelia, and also in a number of epidermal cell types, including those with sensory functions. Earthworms are able to sense and respond to the presence of low concentrations of AgNPs in soils (Shoults-Wilson et al., 2011). It may be a promising line for future investigations to assess if such ciliated cells could be implicated in AgNP detection, internalization or, consequentially, the expression of modified signalling pathways.

4.4. A system toxicology overview of AgNPs vs Ag ions

Uncertainty exists around whether the mechanisms of action of metal and metal oxide NPs and their constituent ions differ, and also which of them are relevant for various considerations in risk assessment, such as the nature of potentially vulnerable species, potential indicators of exposure and the prediction of potential mixture effects. For NPs subject to dissolution, such as Ag, the production of ions from the NPs either outside or inside the organism is a further complication for mechanisms of action assessments *in vivo*. For the AgNPs studied, the toxic effects observed are most likely to be due to a combination of the NPs and the released metal ions (Garcia-Reyero et al., 2014 and references). By generating a well-represented transcriptome for *E. fetida*, a commonly used model in soil toxicology, we have explored the extent to which there is a common mechanism of action between the two Ag forms.

Our initial genetic analysis highlighted the importance of genotyping individuals used for ecotoxicology studies prior to transcriptomic analysis since commercially available organisms may come from genetically mixed cultures that could affect the final results and conclusions of the study. Using AgNP and Ag ion exposed individuals from a single genetic lineage we were able to establish a consistent picture of response to the different Ag forms. The picture is of different uptake mechanisms and toxicokinetics for the two forms, with the AgNPs interacting specifically with cell surface components involved in endocytosis and cilia function. Different internalisation routes, however, ultimately lead to the same mechanistic effects dominated by changes in sugar metabolism and electron transport, protein turnover and DNA conformation. All together may point to an intracellular dissolution of the AgNPs once within tissues. The common toxicodynamic effects observed points to a similar intracellular presence of the active portion of the internalised Ag, most likely as ions that interact with the relevant cellular metal homeostasis machinery, as well as with cellular targets, to cause these toxic effects. This does not preclude that some Ag may still exist within the tissues in NP form, but it suggests that there are no direct or specific toxic effects exerted by such potentially internalised NP forms through pathways not already affected by exposure to ionic Ag.

Acknowledgements

MN, MD and MM were supported by Marie Curie Fellowships, FP7-IEF-GA-2012-329690, FP7-IEF-GA-2010-273207, FP7-IEF-GA-2011-303140. Remaining authors were supported by NanoFATE, Project-CP-FP-247739 under FP7-NMP-ENV-2009, Theme-4; www.nanofate.eu. DJS, CS, EL received core funding from NERC.

Appendix A. Supplementary information

Supplementary information related to this article can be found at http://dx.doi.org/10.1016/j.envpol.2015.07.010.

References

AshaRani, P.V., Hande, M.P., Valiyaveettil, S., 2009. Anti-proliferative activity of silver nanoparticles. BMC Cell Biol. 10.
Baker, T.J., Tyler, C.R., Galloway, T.S., 2014. Impacts of metal and metal oxide nanoparticles on marine organisms. Environ. Pollut. 186, 257–271.
Baylay, A.J., Spurgeon, D.J., Svendsen, C., Griffin, J.L., Swain, S.C., Sturzenbaum, S.R., Jones, O.A.H., 2012. A metabolomics based test of independent action and concentration addition using the earthworm Lumbricus rubellus. Ecotoxicology 21 (5), 1436–1447.
Benmerah, A., 2013. The ciliary pocket. Curr. Opin. Cell Biol. 25 (1), 78–84.
Bianchini, A., Playle, R.C., Wood, C.M., Walsh, P.J., 2005. Mechanism of acute silver toxicity in marine invertebrates. Aquat. Toxicol. 72 (1–2), 67–82.
Buckley, T.R., James, S., Allwood, J., Bartlam, S., Howitt, R., Prada, D., 2011. Phylogenetic analysis of New Zealand earthworms (Oligochaeta: Megascolecidae) reveals ancient clades and cryptic taxonomic diversity. Mol. Phylogenet. Evol. 58 (1), 85–96.
Bundy, J.G., Sidhu, J.K., Rana, F., Spurgeon, D.J., Svendsen, C., Wren, J.F., Sturzenbaum, S.R., Morgan, A.J., Kille, P., 2008. 'Systems toxicology' approach identifies coordinated metabolic responses to copper in a terrestrial non-model invertebrate, the earthworm Lumbricus rubellus. BMC Biol. 6.
Choi, A.O., Brown, S.E., Szyf, M., Maysinger, D., 2008. Quantum dot-induced epigenetic and genotoxic changes in human breast cancer cells. J. Mol. Med. JMM 86 (3), 291–302.
Cornelis, G., Doolette, C., Thomas, M., McLaughlin, M.J., Kirby, J.K., Beak, D.G., Chittleborough, D., 2012. Retention and dissolution of engineered silver nanoparticles in natural soils. Soil Sci. Soc. Am. J. 76 (3), 891–902.
Cunha, L., Montiel, R., Novo, M., Orozco-terWengel, P., Rodrigues, A., Morgan, A.J., Kille, P., 2014. Living on a volcano's edge: genetic isolation of an extremophile terrestrial metazoan. Heredity 112 (2), 132–142.
Dallinger, R., Hockner, M., 2013. Evolutionary concepts in ecotoxicology: tracing the genetic background of differential cadmium sensitivities in invertebrate lineages. Ecotoxicology 22 (5), 767–778.
Davenport, K., Keeley, F.X., 2005. Evidence for the use of silver-alloy-coated urethral catheters. J. Hosp. Infect. 60 (4), 298–303.
Diez-Ortiz, M., Lahive, E., George, S., Ter Schure, A., Van Gestel, C.A., Jurkschat, K., Svendsen, C., Spurgeon, D.J., 2015. Short-term soil bioassays may not reveal the

full toxicity potential for nanomaterials; bioavailability and toxicity of silver ions (AgNO3) and silver nanoparticles to earthworm Eisenia fetida in long-term aged soils. Environ. Pollut. 203, 191–198.
Fabrega, J., Fawcett, S.R., Renshaw, J.C., Lead, J.R., 2009. Silver nanoparticle impact on bacterial growth: effect of pH, concentration, and organic matter. Environ. Sci. Technol. 43 (19), 7285–7290.
Farkas, J., Christian, P., Gallego-Urrea, J.A., Roos, N., Hassellov, M., Tollefsen, K.E., Thomas, K.V., 2011. Uptake and effects of manufactured silver nanoparticles in rainbow trout (Oncorhynchus mykiss) gill cells. Aquat. Toxicol. 101 (1), 117–125.
Garcia-Reyero, N., Kennedy, A.J., Escalon, B.L., Habib, T., Laird, J.G., Rawat, A., Wiseman, S., Hecker, M., Denslow, N., Steevens, J.A., Perkins, E.J., 2014. Differential effects and potential adverse outcomes of ionic silver and silver nanoparticles in vivo and in vitro. Environ. Sci. Technol. 48 (8), 4546–4555.
Gomes, T., Pereira, C.G., Cardoso, C., Bebianno, M.J., 2013. Differential protein expression in mussels Mytilus galloprovincialis exposed to nano and ionic Ag. Aquat. Toxicol. 136, 79–90.
Gong, P., Pirooznia, M., Guan, X., Perkins, E.J., 2010. Design, validation and annotation of transcriptome-wide oligonucleotide probes for the oligochaete annelid Eisenia fetida. Plos One 5 (12).
Grabherr, M.G., Haas, B.J., Yassour, M., Levin, J.Z., Thompson, D.A., Amit, I., Adiconis, X., Fan, L., Raychowdhury, R., Zeng, Q.D., Chen, Z.H., Mauceli, E., Hacohen, N., Gnirke, A., Rhind, N., di Palma, F., Birren, B.W., Nusbaum, C., Lindblad-Toh, K., Friedman, N., Regev, A., 2011. Full-length transcriptome assembly from RNA-Seq data without a reference genome. Nat. Biotechnol. 29 (7), 644–U130.
Haanstra, L., Doelman, P., Voshaar, J.H.O., 1985. The use of sigmoidal dose-response curves in soil ecotoxicological research. Plant Soil 84 (2), 293–297.
Hayashi, Y., Heckmann, L.H., Simonsen, V., Scott-Fordsmand, J.J., 2013. Time-course profiling of molecular stress responses to silver nanoparticles in the earthworm Eisenia fetida. Ecotoxicol. Environ. Safe 98, 219–226.
Heggelund, L.R., Diez-Ortiz, M., Lofts, S., Lahive, E., Jurkschat, K., Wojnarowicz, J., Cedergreen, N., Spurgeon, D., Svendsen, C., 2014. Soil pH effects on the comparative toxicity of dissolved zinc, non-nano and nano ZnO to the earthworm Eisenia fetida. Nanotoxicology 8 (5), 559–572.
Hogstrand, C., Wood, C.M., 1998. Toward a better understanding of the bioavailability, physiology and toxicity of silver in fish: implications for water quality criteria. Environ. Toxicol. Chem. 17 (4), 547–561.
Huang, D.W., Sherman, B.T., Lempicki, R.A., 2009. Systematic and integrative analysis of large gene lists using DAVID bioinformatics resources. Nat. Protoc. 4 (1), 44–57.
James, S.W., Porco, D., Decaens, T., Richard, B., Rougerie, R., Erseus, C., 2010. DNA barcoding reveals cryptic diversity in Lumbricus terrestris L., 1758 (Clitellata): resurrection of L. herculeus (Savigny, 1826). PLoS One 5 (12).
King, R.A., Tibble, A.L., Symondson, W.O.C., 2008. Opening a can of worms: unprecedented sympatric cryptic diversity within British lumbricid earthworms. Mol. Ecol. 17 (21), 4684–4698.
Kollef, M.H., Afessa, B., Anzueto, A., Veremakis, C., Kerr, K.M., Margolis, B.D., Craven, D.E., Roberts, P.R., Arroliga, A.C., Hubmayr, R.D., Restrepo, M.I., Auger, W.R., Schinner, R., Grp, N.I., 2008. Silver-coated endotracheal tubes and incidence of ventilator-associated pneumonia - the NASCENT randomized trial. JAMA J. Am. Med. Assoc. 300 (7), 805–813.
Kwak, J.I., Lee, W.M., Kim, S.W., An, Y.J., 2014. Interaction of citrate-coated silver nanoparticles with earthworm coelomic fluid and related cytotoxicity in Eisenia andrei. J. Appl. Toxicol. 34 (11), 1145–1154.
Langmead, B., Trapnell, C., Pop, M., Salzberg, S.L., 2009. Ultrafast and memory-efficient alignment of short DNA sequences to the human genome. Genome Biol. 10 (3).
Lansdown, A.B., 2006. Silver in health care: antimicrobial effects and safety in use. Curr. Probl. Dermatol. 33, 17–34.
Lowry, G.V., Gregory, K.B., Apte, S.C., Lead, J.R., 2012. Transformations of nanomaterials in the environment. Environ. Sci. Technol. 46 (13), 6893–6899.
Martinez-Zamudio, R., Ha, H.C., 2011. Environmental epigenetics in metal exposure. Epigenetics-US 6 (7), 820–827.
Merico, D., Isserlin, R., Stueker, O., Emili, A., Bader, G.D., 2010. Enrichment map: a network-based method for gene-set enrichment visualization and interpretation. PLoS One 5 (11).
Notter, D.A., Mitrano, D.M., Nowack, B., 2014. Are nanosized or dissolved metals more toxic in the environment? A meta-analysis. Environ. Toxicol. Chem. 33 (12), 2733–2739.
Novo, M., Almodovar, A., Diaz-Cosin, D.J., 2009. High genetic divergence of hormogastrid earthworms (Annelida, Oligochaeta) in the central Iberian Peninsula: evolutionary and demographic implications. Zool. Scr. 38 (5), 537–552.
Novo, M., Almodovar, A., Fernandez, R., Trigo, D., Cosin, D.J.D., 2010. Cryptic speciation of hormogastrid earthworms revealed by mitochondrial and nuclear data. Mol. Phylogenet. Evol. 56 (1), 507–512.
OECD, 2004, April 13. Guideline for the Testing of Chemicals. Earthworm Reproduction Test (Eisenia fetida/Eisenia andrei); No. 222. Organisation for Economic Co-operation and Development.
Otomo, P.V., Maboeta, M.S., Bezuidenhout, C., 2013. Inadequate taxonomy and highly divergent COI haplotypes in laboratory and field populations of earthworms used in ecotoxicology. A case study. Afr. Zool. 48 (2), 290–297.
Owen, J., Hedley, B.A., Svendsen, C., Wren, J., Jonker, M.J., Hankard, P.K., Lister, L.J., Sturzenbaum, S.R., Morgan, A.J., Spurgeon, D.J., Blaxter, M.L., Kille, P., 2008. Transcriptome profiling of developmental and xenobiotic responses in a keystone soil animal, the oligochaete annelid Lumbricus rubellus. BMC Genomics 9.
Perez-Losada, M., Eiroa, J., Mato, S., Dominguez, J., 2005. Phylogenetic species delimitation of the earthworms Eisenia fetida (Savigny, 1826) and Eisenia andrei Bouche, 1972 (Oligochaeta, Lumbricidae) based on mitochondrial and nuclear DNA sequences. Pedobiologia 49 (4), 317–324.
Poynton, H.C., Lazorchak, J.M., Impellitteri, C.A., Smith, M.E., Rogers, K., Patra, M., Hammer, K.A., Allen, H.J., Vulpe, C.D., 2011. Differential gene expression in Daphnia magna suggests distinct modes of action and bioavailability for ZnO nanoparticles and Zn ions. Environ. Sci. Technol. 45 (2), 762–768.
Poynton, H.C., Lazorchak, J.M., Impellitteri, C.A., Blalock, B.J., Rogers, K., Allen, H.J., Loguinov, A., Heckrnan, J.L., Govindasmawy, S., 2012. Toxicogenomic responses of nanotoxicity in Daphnia magna exposed to silver nitrate and coated silver nanoparticles. Environ. Sci. Technol. 46 (11), 6288–6296.
Robinson, M.D., McCarthy, D.J., Smyth, G.K., 2010. Edger: a bioconductor package for differential expression analysis of digital gene expression data. Bioinformatics 26 (1), 139–140.
Roh, J.Y., Sim, S.J., Yi, J., Park, K., Chung, K.H., Ryu, D.Y., Choi, J., 2009. Ecotoxicity of silver nanoparticles on the soil nematode Caenorhabditis elegans using functional ecotoxicogenomics. Environ. Sci. Technol. 43 (10), 3933–3940.
Römbkea, J., Aira, M., Backeljau, T., Breugelmans, K., Domínguez, J., Funke, E., G, N., Hajibabaei, M., Pérez-Losada, M., Porto, P.G., Schmelz, R., Vierna, J., Vizcaíno, A., Pfenninger, M., 2015. DNA barcoding of earthworms (Eisenia fetida/andrei) from 28 ecotoxicological test laboratories. Appl. Soil Ecol. http://dx.doi.org/10.1016/j.apsoil.2015.02.010.
Schlich, K., Klawonn, T., Terytze, K., Hund-Rinke, K., 2013. Effects of silver nanoparticles and silver nitrate in the earthworm reproduction test. Environ. Toxicol. Chem. 32 (1), 181–188.
Shoults-Wilson, W.A., Zhurbich, O.I., McNear, D.H., Tsyusko, O.V., Bertsch, P.M., Unrine, J.M., 2011. Evidence for avoidance of Ag nanoparticles by earthworms (Eisenia fetida). Ecotoxicology 20 (2), 385–396.
Smoot, M.E., Ono, K., Ruscheinski, J., Wang, P.L., Ideker, T., 2011. Cytoscape 2.8: new features for data integration and network visualization. Bioinformatics 27 (3), 431–432.
Tourinho, P.S., van Gestel, C.A.M., Lofts, S., Svendsen, C., Soares, A.M.V.M., Loureiro, S., 2012. Metal-based nanoparticles in soil: fate, behavior, and effects on soil invertebrates. Environ. Toxicol. Chem. 31 (8), 1679–1692.
Tsyusko, O.V., Hardas, S.S., Shoults-Wilson, W.A., Starnes, C.P., Joice, G., Butterfield, D.A., Unrine, J.M., 2012a. Short-term molecular-level effects of silver nanoparticle exposure on the earthworm, Eisenia fetida. Environ. Pollut. 171, 249–255.
Tsyusko, O.V., Unrine, J.M., Spurgeon, D., Blalock, E., Starnes, D., Tseng, M., Joice, G., Bertsch, P.M., 2012b. Toxicogenomic responses of the model organism Caenorhabditis elegans to gold nanoparticles. Environ. Sci. Technol. 46 (7), 4115–4124.
van Aerle, R., Lange, A., Moorhouse, A., Paszkiewicz, K., Ball, K., Johnston, B.D., de-Bastos, E., Booth, T., Tyler, C.R., Santos, E.M., 2013. Molecular mechanisms of toxicity of silver nanoparticles in Zebrafish embryos. Environ. Sci. Technol. 47 (14), 8005–8014.
Waalewijn-Kool, P.L., Ortiz, M.D., van Straalen, N.M., van Gestel, C.A.M., 2013. Sorption, dissolution and pH determine the long-term equilibration and toxicity of coated and uncoated ZnO nanoparticles in soil. Environ. Pollut. 178, 59–64.
Wilkinson, L.J., White, R.J., Chipman, J.K., 2011. Silver and nanoparticles of silver in wound dressings: a review of efficacy and safety. J. Wound Care 20 (11), 543–549.